Light coupling between vertical III-As nanowires and planar Si photonic waveguides for the monolithic integration of active optoelectronic devices on a Si platform

IVANO GIUNTONI,[1,*] LUTZ GEELHAAR,[1] JÜRGEN BRUNS,[2] AND HENNING RIECHERT[1]

[1]*Paul-Drude-Institut für Festkörperelektronik, Hausvogteiplatz 5-7, 10117 Berlin, Germany*
[2]*Technische Universität Berlin, Fachgebiet Hochfrequenztechnik, Einsteinufer 25, 10587 Berlin, Germany*
[*]*giuntoni@pdi-berlin.de*

Abstract: We present a new concept for the optical interfacing between vertical III-As nanowires and planar Si waveguides. The nanowires are arranged in a two-dimensional array which forms a grating structure on top of the waveguide. This grating enables light coupling in both directions between the components made from the two different material classes. Numerical simulations show that this concept permits a light extraction efficiency from the waveguide larger than 45% and a light insertion efficiency larger than 35%. This new approach would allow the monolithic integration of nanowire-based active optoelectronics devices, like photodetectors and light sources, on the Si photonics platform.

References and Links

1. G. Roelkens, L. Liu, D. Liang, R. Jones, A. Fang, B. Koch, and J. Bowers, "III-V/silicon photonics for on-chip and intra-chip optical interconnects," Laser Photonics Rev. **4**(6), 751–779 (2010).
2. K. Gallo and G. Assanto, "All-optical diode based on second-harmonic generation in an asymmetric waveguide," J. Opt. Soc. Am. B **16**(2), 267–269 (1999).
3. M. Lipson, "Guiding, modulating, and emitting light on Silicon-challenges and opportunities," J. Lightwave Technol. **23**(12), 4222–4238 (2005).
4. Y. Furukawa, H. Yonezu, and A. Wakahara, "Monolithic integration of III-V active devices into silicon platform for optoelectronic circuits," IEICE Trans. Electron. **E91–C**(2), 145–149 (2008).
5. S. Liebich, M. Zimprich, A. Beyer, C. Lange, D. J. Franzbach, S. Chatterjee, N. Hossain, S. J. Sweeney, K. Volz, B. Kunert, and W. Stolz, "Laser operation of Ga(NAsP) lattice-matched to (001) silicon substrate," Appl. Phys. Lett. **99**(7), 071109 (2011).
6. A. Y. Liu, C. Zhang, J. Norman, A. Snyder, D. Lubyshev, J. M. Fastenau, A. W. K. Liu, A. C. Gossard, and J. E. Bowers, "High performance continuous wave 1.3 μm quantum dot lasers on silicon," Appl. Phys. Lett. **104**(4), 041104 (2014).
7. D. Van Thourhout, T. Spuesens, S. K. Selvaraja, L. Liu, G. Roelkens, R. Kumar, G. Morthier, P. Rojo-romeo, F. Mandorlo, P. Regreny, O. Raz, C. Kopp, and L. Grenouillet, "Nanophotonic devices for optical interconnect," IEEE J. Sel. Top. Quantum Electron. **16**(5), 1363–1375 (2010).
8. S. R. Jain, Y. Tang, H.-W. Chen, M. N. Sysak, and J. E. Bowers, "Integrated hybrid silicon transmitters," J. Lightwave Technol. **30**(5), 671–678 (2012).
9. L. Zimmermann, G. B. Preve, K. Voigt, G. Winzer, J. Kreissl, L. Moerl, C. Stamatiadis, L. Stampoulidis, and H. Avramopoulos, "High-precision flip-chip technology for alloptical wavelength conversion using SOI photonic circuit," in *IEEE/LEOS Group IV Photonics Conf.* (2011), pp. 237.
10. B. Snyder, B. Corbett, and P. O'Brien, "Hybrid integration of wavelength-tunable laser with silicon photonic integrated circuit," J. Lightwave Technol. **31**(24), 3934–3942 (2013).
11. T. Mårtensson, C. P. T. Svensson, B. A. Wacaser, M. W. Larsson, W. Seifert, K. Deppert, A. Gustafsson, L. R. Wallenberg, and L. Samuelson, "Epitaxial III-V nanowires on silicon," Nano Lett. **4**(10), 1987–1990 (2004).
12. Y. Zhang, J. Wu, M. Aagesen, and H. Liu, "III-V nanowires and nanowire optoelectronic devices," J. Phys. D Appl. Phys. **48**(46), 463001 (2015).
13. X. Zhang, V. G. Dubrovskii, N. V. Sibirev, and X. Ren, "Analytical study of elastic relaxation and plastic deformation in nanostructures on lattice mismatched substrates," Cryst. Growth Des. **11**(12), 5441–5448 (2011).

14. S. D. Hersee, A. K. Rishinaramangalam, M. N. Fairchild, L. Zhang, and P. Varangis, "Threading defect elimination in GaN nanowires," J. Mater. Res. **26**(17), 2293–2298 (2011).
15. K. Tomioka, T. Tanaka, S. Hara, K. Hiruma, and T. Fukui, "III–V Nanowires on Si substrate: selective-area growth and device applications," IEEE J. Sel. Top. Quantum Electron. **17**(4), 1112–1129 (2011).
16. C. P. T. Svensson, T. Mårtensson, J. Trägårdh, C. Larsson, M. Rask, D. Hessman, L. Samuelson, and J. Ohlsson, "Monolithic GaAs/InGaP nanowire light emitting diodes on silicon," Nanotechnology **19**(30), 305201 (2008).
17. W. Wei, X.-Y. Bao, C. Soci, Y. Ding, Z. L. Wang, and D. Wang, "Direct heteroepitaxy of vertical InAs nanowires on Si substrates for broad band photovoltaics and photodetection," Nano Lett. **9**(8), 2926–2934 (2009).
18. R. Chen, T.-T. D. Tran, K. W. Ng, W. S. Ko, L. C. Chuang, F. G. Sedgwick, and C. Chang-Hasnain, "Nanolasers grown on silicon," Nat. Photonics **5**(3), 170–175 (2011).
19. E. Dimakis, U. Jahn, M. Ramsteiner, A. Tahraoui, J. Grandal, X. Kong, O. Marquardt, A. Trampert, H. Riechert, and L. Geelhaar, "Coaxial multishell (In,Ga)As/GaAs nanowires for near-infrared emission on Si substrates," Nano Lett. **14**(5), 2604–2609 (2014).
20. T. Stettner, P. Zimmermann, B. Loitsch, M. Döblinger, A. Regler, B. Mayer, J. Winnerl, S. Matich, H. Riedl, M. Kaniber, G. Abstreiter, G. Koblmüller, and J. J. Finley, "Coaxial GaAs-AlGaAs core-multishell nanowire lasers with epitaxial gain control," Appl. Phys. Lett. **108**(1), 011108 (2016).
21. F. Van Laere, G. Roelkens, M. Ayre, J. Schrauwen, D. Taillaert, D. Van Thourhout, T. F. Krauss, and R. Baets, "Compact and highly efficient grating couplers between optical fiber and nanophotonic waveguides," J. Lightwave Technol. **25**(1), 151–156 (2007).
22. H. Kim, A. C. Farrell, P. Senanayake, W.-J. Lee, and D. L. Huffaker, "Monolithically integrated InGaAs nanowires on 3D structured silicon-on-insulator as a new platform for full optical links," Nano Lett. **16**(3), 1833–1839 (2016).
23. A. F. Oskooi, D. Roundy, M. Ibanescu, P. Bermel, J. D. Joannopoulos, and S. G. Johnson, "MEEP: A flexible free-software package for electromagnetic simulations by the FDTD method," Comput. Phys. Commun. **181**(3), 687–702 (2010).
24. S. K. Selvaraja, W. Bogaerts, P. Absil, D. Van Thourhout, and R. Baets, "Record low-loss hybrid rib / wire waveguides for silicon photonic circuits," in *IEEE/LEOS Group IV Phot. Conf.* (2010).
25. E. D. Palik, *Handbook of Optical Constants of Solids* (Academic Press, Inc., 1985).
26. L. Vj, J. Oh, A. P. Nayak, A. M. Katzenmeyer, K. H. Gilchrist, S. Grego, N. P. Kobayashi, S.-Y. Wang, A. A. Talin, N. K. Dhar, and M. S. Islam, "A pespective on nanowire photodetectors: current status, future challenges, and opportunities," IEEE J. Sel. Top. Quantum Electron. **17**(4), 1002–1032 (2011).
27. L. C. Chiu, J. S. Smith, S. Margalit, A. Yariv, and A. Y. Cho, "Applications of internal photoemission from quantum-well and heterojunction superlattices to infrared photodetectors," Infrared Phys. **23**(2), 93–97 (1983).
28. X. Dai, S. Zhang, Z. Wang, G. Adamo, H. Liu, Y. Huang, C. Couteau, and C. Soci, "GaAs/AlGaAs nanowire photodetector," Nano Lett. **14**(5), 2688–2693 (2014).
29. N. Erhard, S. Zenger, S. Morkötter, D. Rudolph, M. Weiss, H. J. Krenner, H. Karl, G. Abstreiter, J. J. Finley, G. Koblmüller, and A. W. Holleitner, "Ultrafast photodetection in the quantum wells of single AlGaAs/ GaAs-based nanowires," Nano Lett. **15**(10), 6869–6874 (2015).
30. L. Vivien, A. Polzer, D. Marris-Morini, J. Osmond, J. M. Hartmann, P. Crozat, E. Cassan, C. Kopp, H. Zimmermann, and J. M. Fédéli, "Zero-bias 40Gbit/s germanium waveguide photodetector on silicon," Opt. Express **20**(2), 1096–1101 (2012).
31. A. C. Scofield, S.-H. Kim, J. N. Shapiro, A. Lin, B. Liang, A. Scherer, and D. L. Huffaker, "Bottom-up photonic crystal lasers," Nano Lett. **11**(12), 5387–5390 (2011).

1. Introduction

Optical interconnects have been proposed for future technology generations in Si microelectronics, because limitations in bandwidth of electrical interconnects are predicted to become a serious bottleneck [1]. This perspective is supported by the strong expansion of the research and development experienced in the last decade in the field of integrated Si photonics. The achievable large bandwidth and small footprint make this technology appealing not only for transceivers in optical telecommunication but also for on-chip and chip-to-chip interconnects, in particular fast data bus transfer and clock distribution. Recently, the feasibility of a single-chip microprocessor that makes use of direct optical data transfer has been demonstrated [2], showing that functional electronics and optical waveguides can be fabricated on the same chip.

To this end, electronics and optics need to be integrated on the same Si platform. For guiding light, Si is actually an ideal material and the realization of different optical passive components based on Si waveguides can nowadays be considered state of the art (Si photonics) [3]. However, Si as a standalone material is not sufficient for the achievement of active components like light sources and very fast photodiodes. Thus, the combination with

other materials is necessary in order to integrate light sources and detectors on the Si platform. In particular the compound semiconductor classes group-III-arsenides and -phosphides are under consideration, since they offer direct bandgaps of an energy where Si is transparent and can be employed for light guiding.

The integration of these materials on Si is, however, not trivial, because of the large mismatch in lattice constants and thermal expansion coefficients. This mismatch leads for planar growth to the generation of a large number of dislocations that degrade device performance [4]. In order to overcome these limitations, different integration techniques have been proposed in the past, like the use of buffer layers for dislocation reduction [5,6], wafer bonding [7, 8], and hybrid integration [9,10]. Even though interesting results have been presented, none of these concepts could demonstrate at the same time device-level material quality, efficient and compact light coupling to waveguides, and the capability for large-scale integration.

In view of these limitations, there is still a strong need for a novel approach to the integration of active III-V components on Si waveguides that would fulfill the indicated requirements. In this context, the direct epitaxial growth of III-V semiconductors on Si is still highly desirable. Recently, new opportunities have been opened up by growing the III-V material in the form of nanowires [11,12], since their nanometer-scaled footprint and the high aspect ratio relax the matching requirements because strain can elastically relax at the free sidewall surfaces and dislocations likely terminate there [13,14]. Furthermore, the nanowire position can be controlled, e.g., by selective area growth processes [15] and the desired doping profiles and heterostructures can be realized during the epitaxial growth, leading to the realization of several optical devices, including light-emitting diodes, lasers, and photodiodes [15–20]. Still, since Si photonics is a planar technology, where light is transported along waveguides in the substrate plane, a mechanism which permits to change the propagation direction of the light signal is required for a complete interconnect link including light source, waveguide and detector. Here, we analyze the optical interaction between vertical nanowires and planar waveguides in order to design usable systems.

2. Principle

A generic schematic of the interconnect concept introduced and analyzed here is presented in Fig. 1. A periodic two-dimensional array of vertical III-V nanowires is grown on top of a Si waveguide fabricated from a silicon-on-insulator (SOI) wafer. In order to accommodate the nanowire rows, the waveguide width is tapered out. The array exhibits different periods Λ_a and Λ_b in the longitudinal (parallel to the waveguide axis) and lateral directions, respectively. For a proper tailoring of the array periods Λ_a and Λ_b as well as the nanowire diameter d_{NW} light is coupled efficiently between waveguide and nanowires, as discussed in detail below.

The presence of nanowires on top of the waveguide introduces variations in refractive index which partially scatter the light guided in the Si waveguide out of the substrate plane. By arranging these perturbations in an ordered way with a periodicity of Λ_a along the waveguide axis, the nanowires act as a grating coupler. Hence, light propagating in the Si waveguide can be vertically coupled out into the nanowires. By the same mechanism, light generated in the nanowires is coupled into the Si waveguide and propagates along the substrate plane. The choice of the lateral period Λ_b permits to create a photonic crystal which prevents light from escaping from the array laterally. By engineering the heterostructure and the doping profile in the III-V nanowires, the desired optoelectronic functionality can be achieved, with a broad range of possible devices that can be obtained, including light sources and photodetectors.
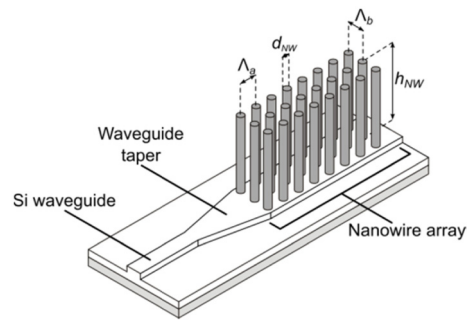
Fig. 1. Generic representation of a periodic array of free-standing III-V nanowires grown on a planar Si waveguide. The waveguide is fabricated from a silicon-on-insulator wafer. The waveguide width is here tapered out to accommodate three parallel rows of nanowires. For a real device, the nanowires would be embedded into a transparent insulating material and electrically contacted. These details are not shown for simplicity.

Grating couplers have been realized so far by etching periodic grooves on the waveguide top surface, e. g. to enable free space light coupling with optical fibers [21]. In the approach described here, the waveguide is kept unaltered, material is added on top of it, and to this material light is directly coupled. Thus, in this approach the nanowires satisfy two different functionalities simultaneously: They act as diffraction grating and at the same time as the active optical component, without requiring additional alignment and mounting steps. The success of the described concept requires the reliable control of the growth position of the nanowires. How this can be achieved exceeds the scope of this paper, which is intended to be general and independent of specific growth processes. Several research groups, however, demonstrated the successful selective area growth of nanowires on Si [15], which is a positive premise for our calculations presented in the following. The feasibility of fabricating regular III-V nanowire arrays on a Si waveguide was recently demonstrated [22]. However, in that study the influence of the array design on the light coupling between nanowires and waveguide was not addressed.

3. Simulations

For an in-depth analysis of the optical interface between nanowires and waveguide, we have performed numerical simulations using the finite difference time domain (FDTD) package Meep [23]. In order to make the analysis applicable to a realistic case, we have considered as basis optical platform the sub-wavelength scaled technology developed in the last years. Here nano-rib waveguides with a rib height of 220 nm are employed, exhibiting a low propagation loss down to 0.3 dB/cm at a wavelength of 1.55 μm [24] and permit hence to realize very compact devices. Also, their small size guarantees a sufficient evanescent field for the realization of coupling structures.

All calculations have been carried out for operation at a wavelength of 1.3 μm. This wavelength is the second standard for data communication beside the wavelength of 1.55 μm. The latter one is the one most commonly used in Si photonics, but also more difficult to achieve for optoelectronic devices based on nanowires made of group-III-arsenides, the archetypical class of compound semiconductors considered here for exemplification. Since in interconnect applications data has to be transmitted only over fairly short distances, the wavelength of 1.3 μm is equally suited and has been chosen for the current analysis. All the refractive indexes used to describe the involved materials have been evaluated at this wavelength: $n_{Si} = 3.504$, $n_{SiO2} = 1.466$, and $n_{GaAs} = 3.406$ [25]. The coupling principle to be demonstrated by these simulations can naturally be transferred to other material systems and wavelengths by properly adjusting dimensions.

For this paper both two- (2D) and three-dimensional (3D) simulations have been carried out. At first sight it would seem obvious that a 3D model is needed for describing the geometry presented in Fig. 1. However, the computation complexity and the memory requirements for such calculations are large enough to make the consideration of a wide range of structural parameters for the nanowire array fairly unfeasible. The reduction to a 2D model by representing the full 3D structure by its cross section would allow to keep the computation complexity moderate and facilitate the evaluation of more parameter variations. Since the nanowire array and the tapered waveguide exhibit a width of the same order of magnitude, the third dimension does not contribute significantly to the coupling effect, but only to the lateral light confinement. Thus, we expect the 2D model to be adequate for the indicated purpose.
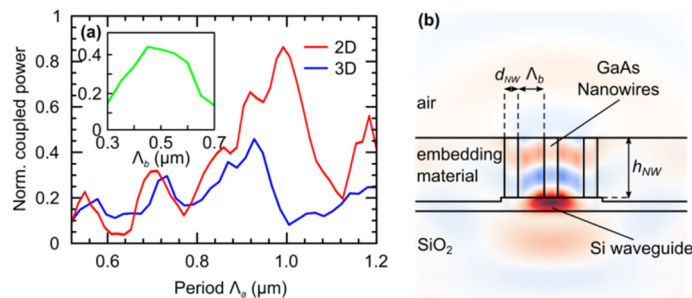

Fig. 2. (a) Calculated dependence of the out-coupled light power, normalized to the power of the light guided in the waveguide, on the array period Λ_a for fifteen periods of nanowires with a fixed height $h_{NW} = 1$ µm and diameter $d_{NW} = 250$ nm. The red curve was calculated with a 2D model, while the blue one with a 3D model. In the inset plot for the 3D case the dependence of the maximum coupling ratio on the lateral period Λ_b is shown. The 3D calculations in the main diagram were carried out for the optimum value $\Lambda_b = 0.45$ µm, considering TE polarization and a waveguide width of 1.7 µm. (b) Computed electric field propagating from the waveguide into the optical interface with the nanowire array. Here the lateral cross section is shown. The colored areas show the amplitude of the electric field, with blue and red marking opposite signs. The parameters for the array are: period $\Lambda_a = 0.92$ µm, row spacing $\Lambda_b = 0.45$ µm, nanowire diameter $d_{NW} = 250$ nm, and nanowire height $h_{NW} = 1$ µm.

In order to verify the validity of 2D simulations for describing the geometry presented here, we calculated the light extraction from a waveguide through an array of fifteen GaAs nanowires as a function of the period Λ_a using both a 2D and a 3D model. In Fig. 2(a) the computed out-coupling ratio (power of light out-coupled from the waveguide by the nanowire array normalized to the power of the guided signal) is depicted for both simulation methods as a function of the array period Λ_a for a nanowire diameter $d_{NW} = 250$ nm and height $h_{NW} = 1$ µm. These values are consistent with the nanowire geometry presented, e.g., in Ref [19]. for the realization of light emitting diodes. It is evident that the reduction to two dimensions tends to overestimate the coupling ratio by almost a factor of two, since the light scattering in the lateral direction is not taken into account. However, the 2D approach still allows to correctly describe the dependence between coupling ratio and array period. The slight difference between the period values where the maximum coupling ratio occurs for the 2D and 3D calculation can be explained by the lower effective refractive index seen by the light signal in the 3D case. For that case, a proper value of the lateral period Λ_b has to be identified as well to achieve a good vertical out-coupling and minimize the light scattering to the sides. The inset plot in Fig. 2(a) depicts how the coupling ratio varies with Λ_b. At a value of $\Lambda_b = 0.45$ µm a lateral photonic crystal is achieved and the lateral propagation is suppressed, maximizing the out-coupling ratio. As shown in Fig. 2(b), light is coupled out and vertically guided through the nanowire array. In view of this comparison, we conclude that calculations performed with a 2D model allow a qualitative description of the optical interface between nanowires and waveguide. Quantitative information requires a full 3D calculation. We thus find it reasonable to explore in the following sections the full dependence of our light-

coupling concept on the choice of the various array parameters with the 2D model. Only in a few exemplary cases where quantitative estimations are required, we provide additional results of 3D calculations to assess absolute efficiencies.
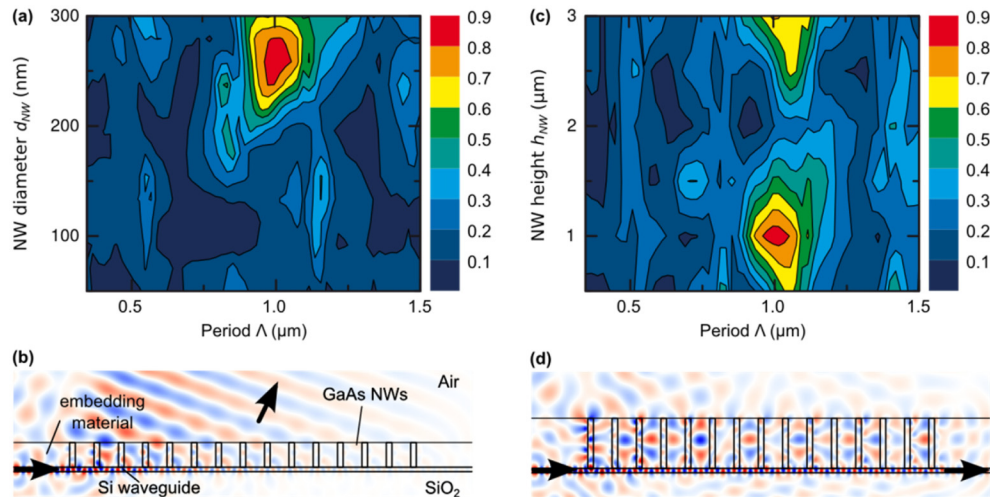

Fig. 3. Out-coupling of light from a Si waveguide resulting from scattering at an array of GaAs nanowires. (a) Calculated dependence of the out-coupled light power, normalized to the power of the light guided in the waveguide, on the array period Λ_a and nanowire diameter d_{NW} for a fixed nanowire height $h_{NW} = 1$ μm. (b) Computed electric field propagating from the waveguide into the optical interface with the nanowire array. The bold black arrows indicate the direction of the phase fronts. The colored areas show the amplitude of the electric field, with blue and red marking opposite signs. The parameters for the array are: period $\Lambda_a = 1$ μm, nanowire diameter $d_{NW} = 250$ nm, and nanowire height $h_{NW} = 1$ μm. (c) Calculated dependence of the out-coupled power, normalized to the power of the light guided in the waveguide, on the array period Λ_a and nanowire height h_{NW} for a fixed nanowire diameter $d_{NW} = 250$ nm. (d) Same as (b), with $h_{NW} = 2$ μm.

An efficient optical coupling interface should be able to transfer as much power as possible from the planar Si waveguide to the nanowires, and viceversa. Hence, a set of different calculations has been performed by varying the period Λ_a of the nanowire array, the diameter d_{NW} and the height h_{NW} of the nanowires (see Fig. 1), and computing the coupled optical power. To do this, an array of 15 periodically aligned GaAs nanowires has been considered. The nanowires are embedded in a polymeric layer with a refractive index analogous to SiO_2 for mechanical stability and planarization that would facilitate hypothetical processing steps like contact deposition. Within the present analysis only the grating functionality of the nanowire array has been tested, i.e. it is considered only if light propagating in the waveguide can be coupled out and externally detected or if impinging light can be coupled into the waveguide. For this purpose, no heterostrucuters in the nanowires have been considered, since their effect on the pure coupling is negligible. The coupling with nanowires with heterostructures for practical use will be discussed in the next sections.

First, the nanowire height has been kept constant to a value of $h_{NW} = 1$ μm. In Fig. 3(a) the out-coupling ratio is depicted as a function of the array periodicity and nanowire diameter. The grating condition is fulfilled for periods in the range 0.9–1.1 μm and diameters between 220 nm and 270 nm. In this region light is almost vertically refracted and out-coupled from the waveguide. At a value of $\Lambda_a = 1$ μm and $d_{NW} = 250$ nm the maximal out-coupling value is reached, with almost 85% of the input light vertically extracted. This coupling can be seen in detail in Fig. 3(b), where the computed electric field for the given geometric parameters is depicted. Light is almost vertically refracted and propagates through the nanowires; the phase fronts of the vertically propagating light exhibit a tilt of about 20° from the normal direction.

The influence of the nanowire height h_{NW} on the out-coupling ratio has been considered as well, keeping the nanowire diameter constant at the value of 250 nm. As it can be observed in Fig. 3(c), the out-coupled power does not increase linearly with the nanowire height, but exhibits maxima for $h_{NW} = 1$ µm and $h_{NW} = 3$ µm. For nanowire heights between the two maxima, the refracted light propagates along the nanowire array and is partially re-coupled to the waveguide [see Fig. 3(d)]. This re-coupling can be explained by considering that the extracted light propagates vertically with different wave vectors in the nanowires and in the embedding material. If the two waves are in phase at the interface to air, light extraction can be externally detected. In contrast, if the waves are out of phase, destructive interference occurs, and no light is extracted from the array. It can therefore be deduced that an optimal light extraction of 85% from the waveguide can be achieved with a nanowire array exhibiting a period $\Lambda_a = 1$ µm, a diameter $d_{NW} = 250$ nm and a height $h_{NW} = 1$ µm. This value is transferred into an extraction ratio of 45% for the full 3D simulation [see Fig. 2(a)].
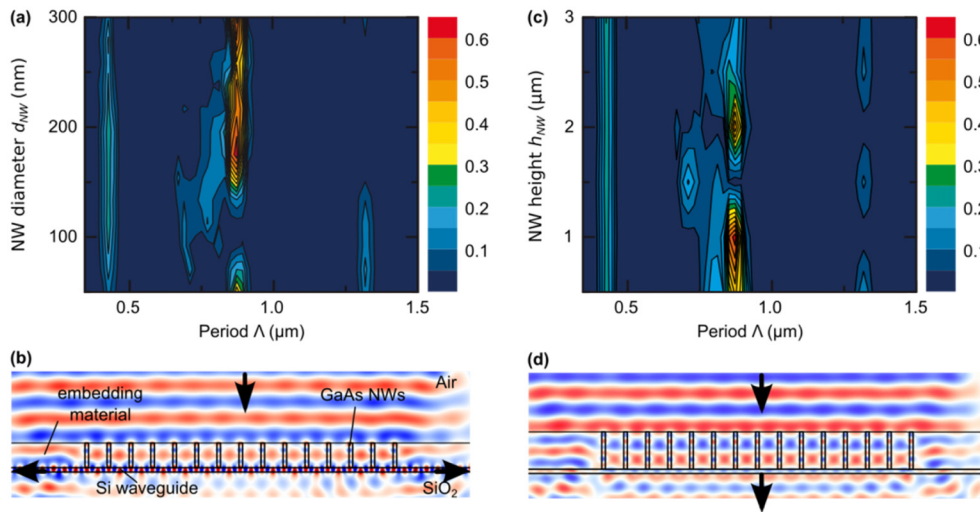

Fig. 4. In-coupling of plane light waves into a Si waveguide resulting from scattering at an array of GaAs nanowires. (a) Calculated dependence of the in-coupled light power, normalized to the power of the impinging light, on the array period Λ_a and nanowire diameter d_{NW} for a fixed nanowire height $h_{NW} = 1$ µm. (b) Calculated dependence of the in-coupled power, normalized to the power of the impinging light, on the array period Λ_a and nanowire height h_{NW} for a fixed nanowire diameter $d_{NW} = 170$ nm. (c) Computed electric field propagating from above the nanowire array into the optical interface with the waveguide. The bold black arrows indicate the direction of the phase fronts. The colored areas show the amplitude of the electric field, with blue and red marking opposite signs. The parameters for the array are: array period $\Lambda_a = 0.87$ µm, nanowire diameter $d_{NW} = 170$ nm, and nanowire height $h_{NW} = 1$ µm. (d) Same as (c), with $h_{NW} = 1.5$ µm.

Since the coupling interface presented here is desired to work in both directions, the reversed situation has been analyzed as well. An optical planar wave impinging orthogonally on the nanowire array has been considered, and the fraction of power coupled to the waveguide has been computed. Similarly to the out-coupling scenario, in Figs. 4(a) and 4(c) the resulting in-coupling efficiency is shown as function of the array period and nanowire diameter and nanowire height, respectively. It can be observed that almost 60% of the impinging light is coupled to the planar Si waveguide through the nanowire array at a period $\Lambda_a = 0.87$ µm, a diameter $d_{NW} = 170$ nm, and a height $h_{NW} = 1$ µm. In the full 3D geometry the corresponding value is around 30%. Also for the in-coupling scenario, the efficiency of the light transfer to the waveguide does not vary linearly with the nanowire height. It exhibits a main maximum at $h_{NW} = 1$ µm and a side maximum at $h_{NW} = 2$ µm, while it reaches a minimum at $h_{NW} = 1.5$ µm. The computed electric field for the configuration corresponding to

the maximum in-coupling efficiency is depicted in Fig. 4(b). In the waveguide light propagates in both directions away from the nanowire array. In Fig. 4(d) one sees the computed electric field for the configuration corresponding to the minimum in-coupling efficiency. Here, waves propagating in the nanowires and in the embedding material impinge on the Si interface out of phase, and hence no light is coupled into the waveguide.

In Fig. 5(a) the spectral bandwidth of the coupling efficiency is plotted for both directions. Here, the nanowire configurations previously identified for the optimum coupling have been considered. The diagram reveals that the light extraction is not only more efficient than light insertion, but also possible over a larger bandwidth. This finding is consistent with the fact that in Figs. 3(a) and 3(c) the maxima are much broader than in Figs. 4(a) and 4(c). The light out-coupling occurs over a bandwidth of $\Delta\lambda_{3dB} = 320$ nm, while the in-coupling over only $\Delta\lambda_{3dB} = 60$ nm. In terms of fabrication, this difference translates into more relaxed patterning tolerances for the former case.

As concluding point, the influence of the number of nanowires in the array on the coupling efficiency has been considered. As it is depicted in Fig. 5(b), the amount of coupled power increases for larger arrays, but not linearly with the number of nanowires. A saturation level is reached for 15 nanowires in the out-coupling and for 20 nanowires in the in-coupling configuration. This result implies that for actual devices a moderate number of nanowires in the array suffices, which means that a fairly compact size can be achieved.
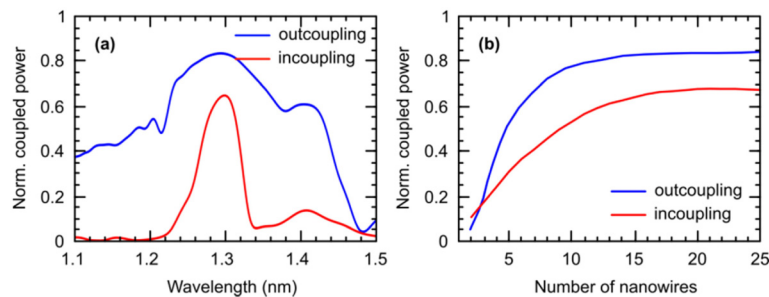

Fig. 5. (a) Calculated spectral bandwidth for the light coupling between nanowires and waveguides in both directions. (b) Dependence of the coupled optical power on the number of nanowires in the array. For the out-coupling scenario a nanowire array with $\Lambda_a = 1$ µm, $d_{NW} = 250$ nm, and $h_{NW} = 1$ µm has been considered, while for the in-coupling scenario the used parameters are $\Lambda_a = 0.87$ µm, $d_{NW} = 170$ nm, and $h_{NW} = 1$ µm.

4. Integration of photodetectors

The ability of the nanowire array to extract light from the waveguide could be employed for the monolithic integration of photodetectors. Nanowires, especially in a core-shell configuration, exhibit several advantages for light detection, since they permit to combine a thin absorbing region with a large lateral surface. Light propagates along the nanowire axis and can therefore be absorbed over a long path through a large lateral surface. The absorbing shell can hence be kept thin, reducing the carrier transit time and leading to higher detector speed [26].

For an efficient light detection, the light out-coupled from the Si waveguide needs to be absorbed in the nanowires. Hence, simulations have been carried out to evaluate the fraction of the light actually absorbed in the array. To this end, coaxial GaAs nanowires including an $In_{0.35}Ga_{0.65}As$ shell as absorbing material have been considered. For the (In,Ga)As shell an absorption coefficient of $\alpha = 10^4$ cm^{-1} has been assumed, the tabulated value for bulk material. In strained layers this value increases slightly, implying higher actual values than calculated here [27]. This absorption has been implemented in the simulation using a complex refractive index for (In,Ga)As of $n = 3.667 + 0.103i$. Since the focus of the present study is on the concept of light coupling between waveguide and nanowires, we refrain from considering

specific device designs. However, beyond the simulations presented in the following, we carried out selected additional calculations aimed at exploring the influence of substrate doping and electrical contacts on system performance. We found that the additional losses compared to the idealized case analyzed in more detail are below 10%.

The computed absorption in an array of 15 nanowires is shown as a function of the period in Fig. 6(a) (d_{NW} = 250 nm, h_{NW} = 1 µm). For comparison, the total out-coupling efficiency of the array is depicted as well [same data as in Fig. 3(a)]. It is clear that for a period of 1 µm, where the maximum of light extraction occurs, also the absorption of the incoming signal has its maximum with a value of 0.2. In order to obtain a more realistic value for the absorption efficiency, the computation has been repeated using the 3D model. These calculations show that a maximal absorption of 0.15 is reachable [dashed lines in Fig. 6(a)]. Thus, the ratio between the absorption efficiencies calculated with the two models is actually significantly smaller than the ratio for the pure light coupling efficiencies. This difference can be attributed to the larger amount of absorbing material rendered in the full array of three rows of 3D core-shell nanowire compared to the simpler 2D cross section.

By increasing the nanowire height and the shell thickness, the achievable absorption can be increased, as shown in Fig. 6(b) with 2D calculations. The overall absorption increases with h_{NW}, taking advantage of the light confinement along the array shown on Fig. 3(d), and reaches values of 60% for a nanowire height of h_{NW} = 3.5 µm and an (In,Ga)As shell thickness of 20 nm.

The results shown in this section demonstrate that our new light coupling concept enables the use of vertical core-shell nanowires as photodetectors for planar Si waveguides. As a matter of fact, recently high performance photodetectors based on core-shell nanowires have been shown [28,29], which could potentially be integrated with Si waveguides. Such nanowire photodetectors would have to compete with the widely spread state-of-the-art Ge photodetectors [30]. However, if light sources based on III-As nanowires were implemented on the same substrate, it would be technologically favorable to realize detectors using the same material system, and the next section is devoted to that topic.
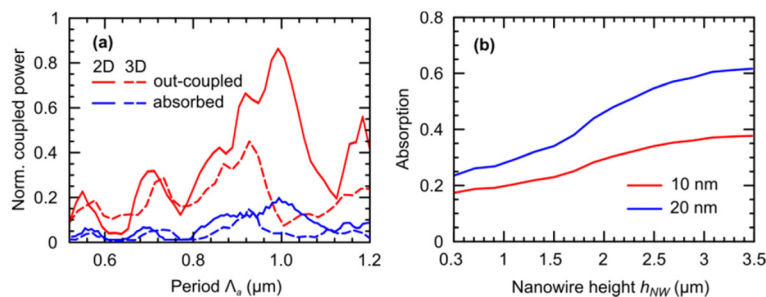

Fig. 6. Light coupling from Si waveguides into GaAs/In$_{0.35}$Ga$_{0.65}$As core-shell nanowires acting as photodetectors. (a) Optical power absorbed in an array of 15 nanowires with diameter d_{NW} = 250 nm, height h_{NW} = 1 µm, and shell thickness 10 nm, compared to the total out-coupled power, both normalized to the power of the light guided in the Si waveguide and plotted as a function of the array period Λ_a for core-shell nanowires acting as photodiodes. The continuous lines indicate calculations performed with a 2D model, dashed lines with a 3D one. (b) Absorption in the nanowire array (Λ_a = 1 µm, d_{NW} = 250 nm) calculated with a 2D model as a function of the nanowire height h_{NW} for two different (In,Ga)As shell thicknesses.

5. Integration of light sources

In order to evaluate our light coupling concept with respect to the use of light emitters based on III-As nanowires, numerical simulations have been performed in which the sources of light have been placed in the nanowires themselves. In principle two different possible light emitters can be achieved with nanowires: light emitting diodes (LED) and lasers. The former ones are easier to fabricate experimentally, but provide only incoherent emission, which is

generally less suitable for signal processing. The latter ones are preferred because of their coherent emission, but require at the same time the realization of an optical resonator. An example of a photonic crystal cavity based on ordered GaAs nanowires is shown in Ref [31].

In Fig. 7(a) the in-coupling efficiency is shown as a function of the array period for the two different cases coherent and incoherent emission in the nanowires, calculated using a 2D model. In the case of coherent emission up to 65% of the generated light can be coupled into the waveguide in both lateral directions at a period Λ_a = 0.87 μm. In the case of incoherent emission, the efficiency is much lower and almost does not vary with the array period. For comparison, the in-coupling efficiency for coherent emission calculated with a 3D model is plotted as well, indicating that up to 35% of the generated light can be coupled into the waveguide in a real device. Figure 7(b) depicts the electric field for coherent emission in the nanowires with a period Λ_a = 0.87 μm, computed for the 2D case. The generated light impinging on the Si surface couples to the fundamental mode of the waveguide and propagates in both horizontal directions. The electric field computed for incoherent emission is finally presented in Fig. 7(c), where it can be observed that the light coupling occurs mostly through scattering, which explains both the reduced efficiency and the independence of the period.

These simulations show that for efficient light coupling a coherent light source is highly desirable: the wave fronts have to be in phase at the nanowire-waveguide interface. However, laser sources are in any case fundamental components for the realization of optical interconnects, so our finding does not impose any tightened requirement. At the same time, our data demonstrate that light from monolithically integrated lasers based on vertical III-As nanowires can be coupled into planar Si waveguides.
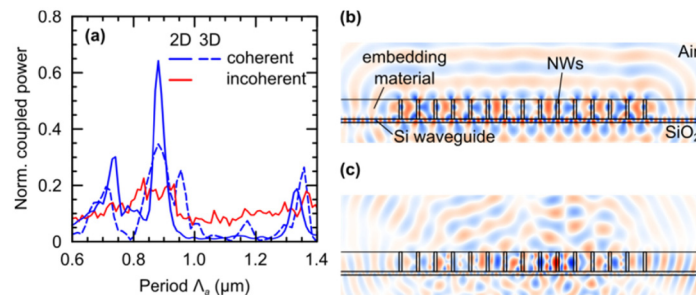

Fig. 7. Light coupling from GaAs nanowires acting as light sources. (a) Calculated dependence of the power coupled into the waveguide, normalized to the power generated in the nanowires, on the array period. Both cases of coherent and incoherent emission are shown. The continuous and dashed blue lines indicate the coupling of coherent emission, calculated with a 2D and 3D model, respectively. An array of 15 nanowires with diameter d_{NW} = 170 nm and height h_{NW} = 1 μm has been considered. Electric field of (b) coherent and (c) incoherent radiation generated in the nanowire array and coupled into the Si waveguide for the period Λ_a = 0.87 nm, computed with a 2D model.

6. Conclusions

Considering an integration concept with vertical III-As nanowires grown on top of planar Si waveguides, our calculations show that light can efficiently couple in both directions between the two different material systems. The concept presented here is not limited to III-As nanowires but can be transferred to other material systems and wavelengths by properly adjusting dimensions. Obtaining high efficiency requires the growth of the nanowires in the shape of a periodic array with suitable geometry. In this case, the nanowire array acts as a grating coupler. If the nanowires are configured as photodetector, the nanowire array can therefore allow both the extraction and detection of light propagating in the waveguide. Alternatively, the nanowires can be employed at the same time for light generation and light coupling into the waveguide. By combining these two components, a complete optical

interconnect system could be realized, which could serve as the basis for future optical on-chip data communication.

Funding